Composite Structures 300 (2022) 116127

Contents lists available at ScienceDirect

Composite Structures

journal homepage: www.elsevier.com/locate/compstruct

Fracture tailoring in 3D printed continuous fibre composite materials using the Phase field approach for fracture

S. Sangaletti *, I.G. García

Grupo de Elasticidad y Resistencia de Materiales, Escuela Técnica Superior de Ingeniería, Universidad de Sevilla, Camino de los Descubrimientos s/n, 41092 Sevilla, Spain

ARTICLE INFO

Keywords:
Additive layer manufacturing
3D printed materials
Phase field
Finite elements

ABSTRACT

Additive Manufacturing is a technology with high potential since it offers a lot of benefits going from lower material waste to flexibility in the component fabrication process. The continuous Carbon Fibre (CF) deposition is an interesting approach since it allows to depose continuous CF bundles following different geometries and avoiding the limitations of current composite manufacturing techniques. Choosing the CF deposition path means also giving the designer the possibility to reinforce areas of the designed component which are subjected to stress concentrations, thus increasing its fracture resistance. In this work, a study on the reinforcement capabilities of this technology is performed, considering different specimen geometries and different geometries for the CF deposition path. Two different geometries are analysed: a V-notch and an Open-Hole specimen, both subjected to tensile loading. To model the fracture scenario, a Phase Field framework is exploited. The V-notch simulation demonstrates the capability of Phase Field to catch both the fracture path and the mechanical response reported in experiments from the literature. In the second part of the paper, the Open Hole Tension test is simulated numerically by means of the same tools described above, taking into consideration different geometries for the reinforcement around the hole. The specimens with different reinforcement geometries show different mechanical responses and crack patterns, thus highlighting the influence of the continuous CF reinforcement geometry on the fracture scenario.

1. Introduction

In the recent years, Additive Manufacturing (AM) has captured more and more interest among both industrial and academic players due to the opportunities that this technology offers. Among the main advantages given by this fabrication technique, the following can be surely listed: (1) Flexibility of the process, allowing the fabrication of components without the use of molds; (2) Generation of components of arbitrary and complex shapes, as a consequence of the previous point; (3) Reduced material waste and (4) Application to the composite materials scenario.

Among all the advantages just listed above, the last one is the most interesting for mechanical and structural applications. While 3D printing of polymeric materials is a consolidated approach, widely studied in literature, 3D printing of Carbon Fibre (CF) reinforced polymers is currently under study. The possibility of deposing continuous CF along with common polymeric material allows the designer to give particular attention to areas of the component which could be subjected to higher stresses for whichever reason (notches, discontinuities, loading geometry) [1]. The reinforcement of such areas with CF allows a better resistance to phenomena like fracture which could lead to the catastrophic failure of the component. That is why this deposition technique is of particular interest and object of study in this article. For the sake of clarity, when it is said continuous CF deposition, it means that a bundle of fibres is deposed along a defined path, not a single fibre.

The mechanical behaviour of 3D printed CF reinforced polymers has been studied in the most recent years by different authors: Pertuz et al. [2] printed different specimens reinforced with CF, Glass Fiber and Kevlar to study both their static and fatigue behaviour. Caminero et al. [3] focused the attention on the effect of the layer thickness and fibre volume fraction on the interlaminar bonding behaviour of printed specimens reinforced with CF, Glass Fiber and Kevlar. In another work [4], the same authors studied the influence of different process parameters on the impact strength of continuous reinforced polymers. Justo et al. [5] showed the increased mechanical properties of coupons reinforced with CF under tensile loading. Dutra et al. [6] studied the tensile and compression properties of such composites, in longitudinal and transverse direction. Akasheh et al. [7] studied the influence of

* Corresponding author.
E-mail addresses: ssangaletti@us.es (S. Sangaletti), israelgarcia@us.es (I.G. García).

https://doi.org/10.1016/j.compstruct.2022.116127
Received 6 June 2022; Received in revised form 26 July 2022; Accepted 13 August 2022
Available online 20 August 2022

the reinforcement on a notched specimen under tension, highlighting the important contribution of the CF reinforcement on the fracture behaviour of the specimen itself. To conclude, Saeed et al. [8] predicted the in-plane mechanical properties of CF reinforced 3D printed polymer composites using the classical laminated-plate theory. Several investigations were also performed on holed 3D printed specimens with continuous fibre reinforcement. Prajapati et al. [9] focused the attention on the open hole tensile strength of such components, testing coupons realized with Onyx polymeric material and Glass Fibre. They observed that the fibre reinforcement increases the tensile strength, at the cost of printing time and coupon's weight. Sanei et al. [10] printed different specimens made of Nylon and reinforced with CF, with different hole dimensions, to test the influence of the reinforcement around the hole, reporting a failure scenario initiating at the stress concentration region but not passing through the hole.

In addition to all the experimental works described so far, numerical ones have been carried out. Some aim at analysing the possible application of optimization techniques that could affect some parameters of the coupon, e.g. its stiffness. Jiang et al. [11] proposed a continuous fibre angle optimization approach in order to compute the best fibre orientation of the 3D printed structure, aligning fibres along the principal loading direction and minimizing the compliance. Safonov et al. [12] adopted another optimization strategy in order to produce a printed structure that, thanks to the introduction of the fibre reinforcement, could be as stiff as the starting one, made of isotropic material, but saving up to 90% of the weight. Other works studied the possible evolution of cracks inside 3D printed materials. Li et al. [13] used Phase Field approach to simulate the crack propagation in 3D polymeric materials, but without taking into consideration the presence of continuous fibres. They used this method to optimize the shape of multimaterial 3D printed specimens subjected to different loading conditions basing the whole analysis on the work done by the external load applied. To the authors' best knowledge, no work has been done so far on the numerical study of crack propagation inside 3D printed materials reinforced with continuous fibres using the Phase Field approach.

The choice of such tool to analyse the crack path relies on its versatility. In fact, other methods lack of efficiency when dealing with complex crack patterns involving branching or coalescence. From this point of view, Phase Field could be able to describe complex phenomena like crack propagation in heterogeneous materials [14]. Details regarding this method can be found in [15,16]. A brief description is included in Section 2. This method has been recently exploited to analyse crack propagation in composite materials. In [17], Phase Field is used to analyse the crack propagation at the microscale inside a ultrathin cross-ply laminate. Matrix and fibres were treated as separated parts, resulting in the prediction of a crack pattern which matches experimental observations: crack runs along fibre-matrix interface and matrix. [18] studied the progressive failure in multi-phase materials, including the case of composite materials. The problem was first studied in 2D and then in 3D in [19]. In [20], the effect of the micro structure on the fracture toughness of fibre-reinforced polymer composites is assessed by means of coupling Phase Field and cohesive zone models. In [21], the same authors always investigate the fracture toughness in such materials, but taking into consideration the effect of fibre bridging. In [22], a multi Phase Field model is proposed to analyse the intra-laminar failure for long fibre reinforced composites relying on Puck's failure criterion. In [23], Phase Field has been used to study the mechanical behaviour of functionally graded material.

In this study, the fracture phenomena in CF reinforced 3D printed specimens are investigated by means of the Phase Field approach. The paper is organized as follows. In Section 2, the Phase Field approach for fracture is presented and described briefly. In Section 3, a first study regarding notched tension specimens is presented. Two different CF deposition paths are taken into account, replicating the tensile tests available in literature. The results of the numerical simulations are compared with the experimental ones obtained by these authors. In Section 4, a study regarding a Open Hole tension specimen is presented. The result of the numerical simulation is compared with the experimental one obtained by other authors and different solutions for the reinforcement of the specimen are proposed, checking how they affect its mechanical behaviour and the crack pattern.

2. Phase field approach for fracture

This section provides a brief description of the Phase Field approach used here to model fracture in 3D printed composite specimens.

The Phase field approach for fracture [15] is based on the variational approach for fracture [24], where the Griffith's criterion for crack propagation is formulated as a variational problem. Considering an arbitrary body $\Omega \in \mathbb{R}^n$ with boundary $\partial\Omega \in \mathbb{R}^{n-1}$, which contains a crack at a line (in 2D) or surface (in 3D) Γ, the total potential energy Π of this body can be expressed as a function of the displacement field $\mathbf{u}$ and the crack topology Γ:

$$\Pi(\mathbf{u},\Gamma) = \Pi_{\text{el}}(\mathbf{u}) + \Pi_{\text{f}}(\Gamma) - \Pi_{\text{ext}}(\mathbf{u}) = \int_{\Omega\setminus\Gamma} \psi^{\text{e}}(\boldsymbol{\varepsilon})\mathrm{d}\Omega + \int_{\Gamma} G_{\text{c}}\mathrm{d}\Gamma - \Pi_{\text{ext}}(\mathbf{u}) \tag{1}$$

where $\psi^{\text{e}}(\boldsymbol{\varepsilon})$ is the elastic energy per unit volume, function of the strain tensor $\boldsymbol{\varepsilon}$, G_{c} is the material fracture toughness and Π_{ext} is the work of external forces. Thus, the first term Π_{el} represents the elastic energy and the second term Π_{f} the fracture energy. In the variational approach for fracture, the equilibrium displacement $\mathbf{u}$ and the crack topology Γ at a certain time step t, assuming displacement control, is given by the minimization of the total potential energy $\Pi(\mathbf{u},\Gamma)$:

$$(\mathbf{u}(t),\Gamma(t)) = \underset{\mathbf{u}=\bar{\mathbf{u}}(t) \text{ on } \partial\Omega_{\mathbf{u}}}{\operatorname{argmin}} \Pi(\mathbf{u},\Gamma) \tag{2}$$

where $\bar{\mathbf{u}}$ is the displacement prescribed at the boundary part with Dirichlet conditions on $\partial\Omega_{\mathbf{u}}$. The solution of this minimization gives the evolution of the displacement field $\mathbf{u}$ and the crack topology Γ over the time t.

Several computational approaches have been proposed to solve the minimization problem in (2). Among them, the variational Phase field approach is used here. It is based on the introduction of a regularization length l to switch from the sharp-crack topology to a diffused one, see Fig. 1. Therefore, the physical crack is regularized with a scalar Phase field variable α which ranges from 0, corresponding to intact material, to 1, corresponding to fully damaged. Adopting this approach and assuming the particular AT-2 functional in the sense [25,26], the fracture energy Π_{f} in (1) is rewritten as,

$$\Pi_{\text{f}}(\alpha) = \int_{\Omega} \gamma(\alpha,\nabla\alpha)\mathrm{d}\Omega = \int_{\Omega} G_{\text{c}}\left(\frac{1}{2l}\alpha^2 + \frac{1}{2}l\,|\nabla\alpha|^2\right)\mathrm{d}\Omega \tag{3}$$

where $\gamma(\alpha,\nabla\alpha)$ is the crack density functional, $\nabla\square$ represents the spatial gradient, and l is the damage characteristic length. This length l is a regularization parameter which modulates the thickness of the damaged region. In summary, this regularization avoids that the minimization of (2) will lead to a damage localization in a zero thickness region, circumventing mesh-sensitivity.

With respect to the elastic energy $\psi^{\text{e}}(\boldsymbol{\varepsilon})$, it is calculated as follows:

$$\psi^{\text{e}}(\boldsymbol{\varepsilon}) := g(\alpha)\left(\frac{1}{2}K\langle\mathrm{tr}(\boldsymbol{\varepsilon})^2\rangle_+ + \mu(\boldsymbol{\varepsilon}_{\text{dev}} : \boldsymbol{\varepsilon}_{\text{dev}})\right) + \frac{1}{2}K\langle\mathrm{tr}(\boldsymbol{\varepsilon})^2\rangle_- \tag{4}$$

where $\mathrm{tr}(\boldsymbol{\varepsilon})$ is the trace of $\boldsymbol{\varepsilon}$, and $\langle\square\rangle_+ = \square$ if $\square \geq 0$ and $\langle\square\rangle_+ = 0$ if $\square < 0$. K and μ are the elastic bulk and shear moduli, respectively. The function $g(\alpha)$ is a degradation function which affects the material behaviour when the damage parameter α increases. In this work, the usual quadratic degradation will be used:

$$g(\alpha) := (1-\alpha)^2 \tag{5}$$

Other degradation functions have been proposed, see [27] for a review.

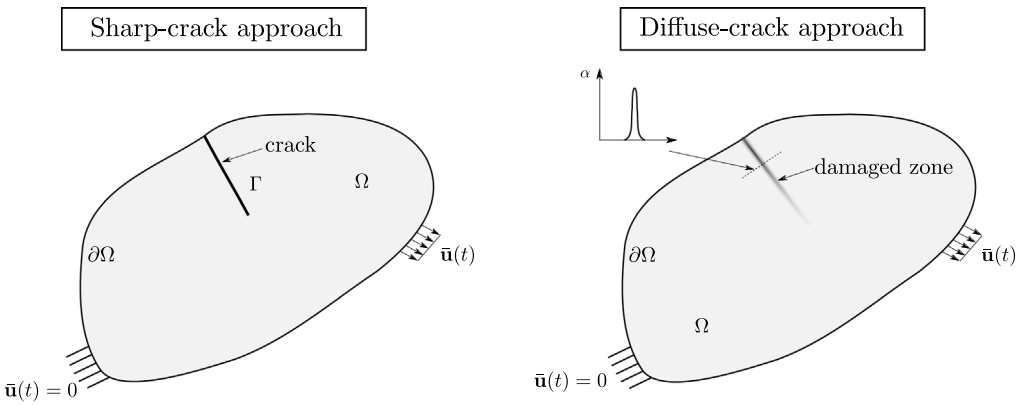

Fig. 1. Schematic of sharp-crack and diffuse-crack approaches in an arbitrary solid with domain Ω and boundary $\partial\Omega$.

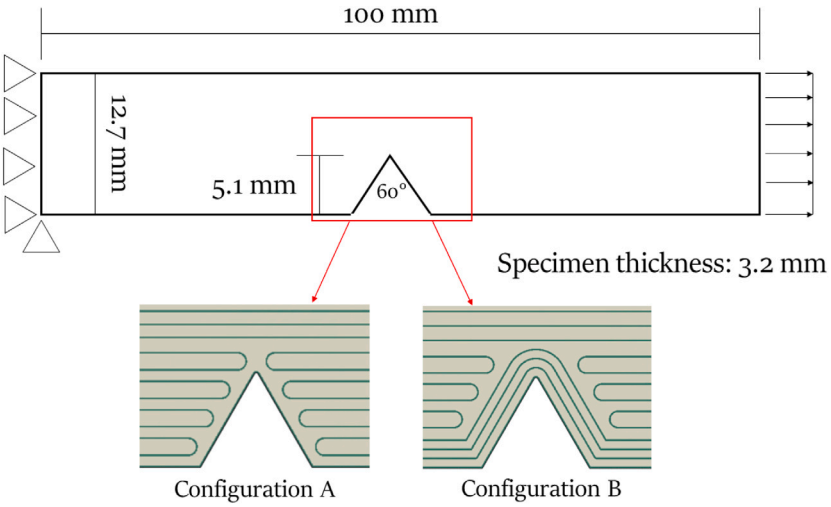

Fig. 2. Notched specimen geometry and boundary conditions. The different reinforcement geometries are shown. Configuration A (left) and Configuration B (right).

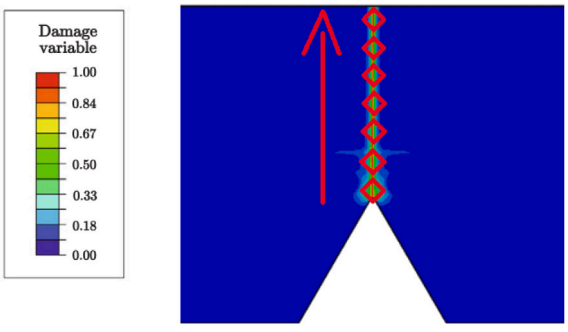

Fig. 3. Crack pattern for the specimen without reinforcement around the notch. Comparison between Phase Field value and experimental results (indicated with red rhombus).

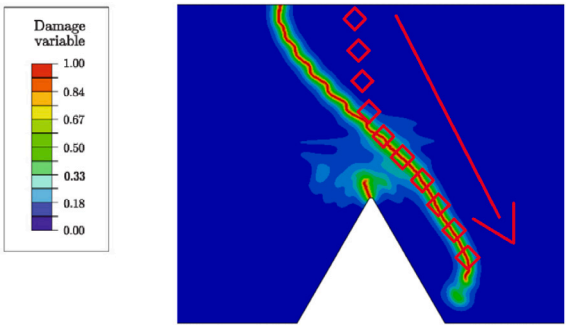

Fig. 4. Crack pattern for the specimen with reinforcement around the notch. Comparison between Phase Field value and experimental results (indicated with red rhombus).

Substituting (4) and (3) in (1), the variational problem in (2) becomes now a variational problem where the variables are the displacement field $\mathbf{u}$ and the damage field $\boldsymbol{\alpha}$:

$$(\mathbf{u}(t), \boldsymbol{\alpha}(t)) = \underset{\mathbf{u}=\bar{\mathbf{u}}(t) \text{ on } \partial\Omega_{\mathbf{u}}}{\operatorname{argmin}} \; \Pi(\mathbf{u}, \boldsymbol{\alpha}) \tag{6}$$

It has been proven that for $l \to 0$, the solution of this problem converges to the classical Griffith's criterion [28,29].

This variational problem in (6) can be implemented in a nonlinear finite elements analysis, being $\mathbf{u}$ and $\boldsymbol{\alpha}$ the degrees of freedom defined at nodes. Many implementations are available in different FE codes. Among them, in this work the implementation in Abaqus/Standard by Navidtehrani et al. [30] is used. The main characteristic of this implementation is that it is implemented in a user subroutine UMAT, which has certain advantages in terms of simplicity of the analysis.

3. V-notched tension specimen: Tailoring the crack pattern

In this section, the capability of Phase Field fracture modelling to predict the crack pattern and mechanical behaviour of 3D printed

Table 1
Material properties.

	E [GPa]	ν	G_c [N/mm]	l [mm]
Onyx	1.4	0.3	30	0.2
CF bundle	54	0.3	60	0.2

components is assessed, analysing the beneficial effect the reinforcement has on their mechanical response. To investigate and validate the performance of Phase Field fracture modelling for CF reinforced 3D printed materials, two numerical models replicating the experimental tests carried out in [7] are considered.

3.1. Computational model

The specimen modelled is a notched rectangular specimen of dimension 100.0 mm × 12.7 mm, with a notch of length 5.1 mm and forming an angle of 60 degrees, see Fig. 2. Boundary conditions and loading direction are shown in the same figure. The specimen is subjected to tensile loading by means of the application of a horizontal displacement. All dimensions and geometry are taken from the experimental work presented in [7].

Two configurations are analysed: configuration A, with no additional CF reinforcement around the stress concentration point, i.e. the notch, in Section 3.2.1 and configuration B, with fibre reinforcement around the notch in Section 3.2.2, replicating the tests reported in [7]. The detail of the two configurations is shown in Fig. 2. Here the Polymer is indicated with a light brown colour, while the CF with a dark green.

In all the models generated, the geometry has been partitioned to take into account the presence of two materials, i.e. the polymer and the CF, replicating the deposition pattern used in the experimental work. The properties of these two materials are shown in Table 1. They were taken from other works: [8] as far as the elastic properties are concerned and from [31,32] for the fracture properties. The CF bundle is considered isotropic since very few information is provided by the producer on such material. Two different meshes were used to check mesh independence. Referring to the length scale l, which has been considered equal for the two materials, as highlighted in Table 1, two mesh sizes were used: a coarse one, with elements dimension four times smaller than l and a fine one, with elements dimension six times smaller than l. In all the cases, a mesh constituted by Plane Stress Abaqus triangular and quadrilateral linear elements has been used. A Phase Field AT2 formulation is used, exploiting the analogy between the Phase Field evolution equation and the Heat transfer equation in the sense of [30]. The result of the mesh comparison is that both the crack pattern and stress–strain curves experience negligible changes with respect to the mesh size. Consequently, the curves and picture used in the comparison between experiments and numerical simulations are the result of the analyses performed with the fine mesh.

3.2. Results

In the following subsections, the results of the numerical simulations performed with the two models are shown, highlighting the correspondence with the experimental results and the difference in the mechanical response.

3.2.1. Configuration A

The results of the analysis of the specimen without reinforcement show good agreement with the experiments of Ref. [7], as shown in Fig. 3. Here the experimental crack pattern and propagation direction are indicated with red rhombus and arrow, respectively. The damage variable ranges from 0 for sound material to 1 for totally damaged material.

The crack starts from the notch and it cuts the specimen open along the vertical direction (perpendicular to the one the displacement is applied along), leading to a sudden failure. This happens despite of the presence of the fibres aligned with the loading direction. Also the comparison between the Stress–Strain curves obtained numerically and experimentally shows good agreement. In Fig. 5 the comparison can be appreciated. The slight difference between numerical results and experiments is due to the fact that the information related to the exact reinforcement and printing geometry is missing. Nevertheless, the main goal of this analysis is to replicate the difference in the behaviour of the two specimens, both from the crack path and mechanical response point of view. Therefore, the results can be considered satisfying.

3.2.2. Configuration B

The results of the analysis of the specimen with CF reinforcement around the notch show again good agreement with the experiments of Ref. [7], as shown in Fig. 4.

In contrast to what happened in the specimen without additional reinforcement, the crack does not propagate from the notch, but from the opposite side. Moreover, the propagation path is not straight and it does not pass by the notch. As can be noticed, once the crack cuts the straight fibres and reaches the notch, the presence of a weaker area only made of polymeric material makes it deviate to follow the edge of the reinforcement. Also in this case, the comparison between the Stress–Strain curves got numerically and experimentally shows good agreement.

The same considerations related to the difference between numerical and experimental results in case of Configuration A apply to Configuration B.

3.3. Comparison and conclusions

A last analysis can be performed by comparing the curves for configuration A and B in Fig. 5. As the authors have noticed from the experimental evidences, there is a relevant difference in the stiffness and strain at failure. It is indeed noticeable that in the case of no reinforcement (Configuration A) the stiffness is higher due to a bigger portion of CF aligned exactly with the loading direction. In the reinforced specimen (Configuration B), as a matter of fact, the additional carbon fibre placement along the notch reduces the space available for the straight fibres, leading to a lower value. Regarding the Strain, the higher value in case of Configuration B highlights the beneficial effect of the reinforcement.

Considering the agreement of numerical and experimental results of the simulations carried out so far, the ability of Phase Field to describe the fracture scenario in CF 3D printed materials is also exploited in the next section where another fracture problem is tackled by means of the same approach.

4. Open Hole specimen: Maximizing strength and fracture toughness

In this section, a typical aeronautical case study is considered, the Open Hole tensile test. The aim of this investigation is to understand whether the usage of a continuous CF reinforcement could be useful to increase the mechanical properties of a holed 3D printed coupon subjected to tensile loading, following the experimental work in [10].

The Open Hole topic is of great importance in the aeronautical field, as the safety of structural joints is of primarily importance. For instance, fuselages are assembled joining different building blocks and, being primary structures, the verification of the integrity of its holes under the operating loads is mandatory. The same can be said for the helicopter industry. The point of attach of each blade to the central hub of the rotor is a very critical region and the bolted connection between these parts (usually two bolts for each blade are used) needs to be verified carefully through ad-hoc tests. The importance of this

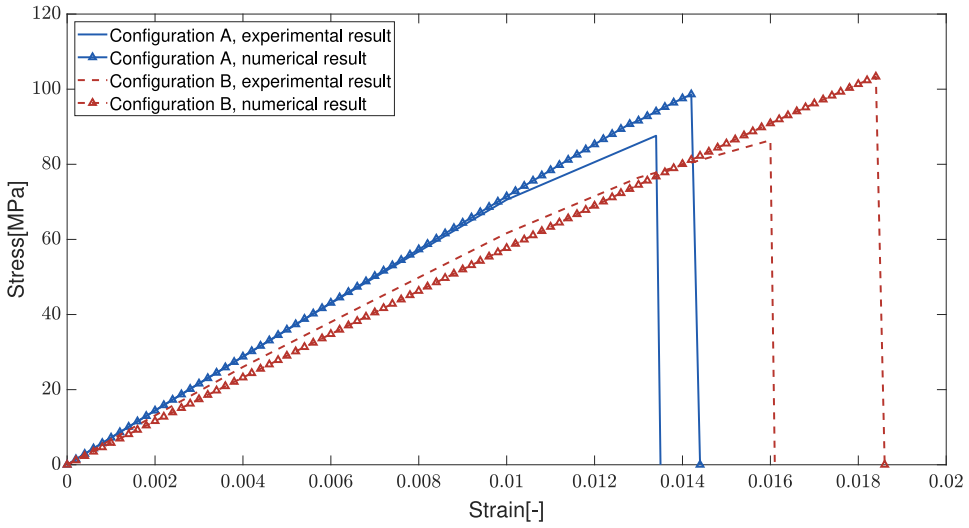

Fig. 5. Comparison between experimental and numerical results for the specimens analysed.

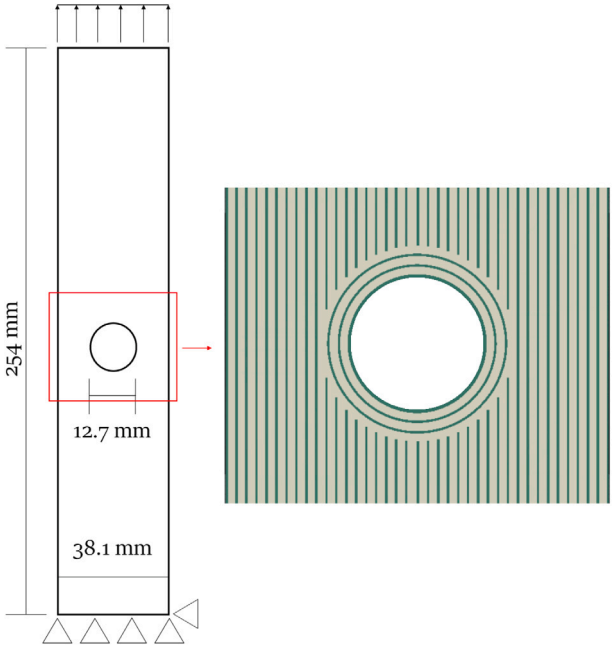

Fig. 6. Holed specimen: tested configuration.

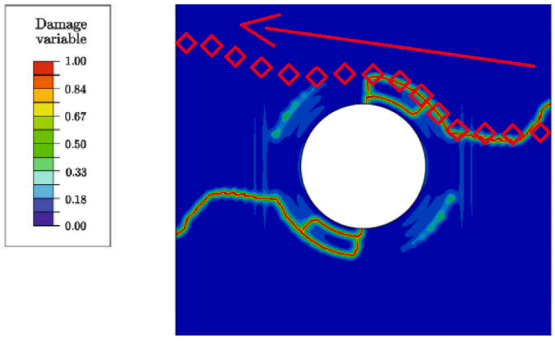

Fig. 7. Holed specimen: comparison between Phase Field value and experimental results (in red).

kind of test is therefore evident. Some authors in the literature showed that the introduction of continuous fibre reinforcement can lead to a great improvement in the mechanical characteristics of additive manufactured materials [12]. It is then of great interest to consider the effect of fibre reinforcement in structural performance enhancement in Open Hole tests, checking if some important results can be obtained, thus leading the way to a possible development of new junctions, lighter and with higher strength and fracture toughness.

In this section, the same configuration studied experimentally in [10] is analysed numerically by means of the Phase Field approach for fracture. In a second part, having verified that the Phase Field is able to correctly catch the crack pattern, some new configurations are tested to check the influence of the CF deposition path both on the crack pattern and mechanical behaviour of the Open Hole specimen. In these analyses, only the geometry of the reinforcement is changed, adopting the same geometrical dimension for the coupon, i.e. height, width and hole diameter.

4.1. Computational model

The model used is a rectangular specimen of dimension 254.0 mm × 38.1 mm with a central hole of 12.7 mm diameter. All dimensions and geometry are taken from the work of [10] and shown in Fig. 6, along with the boundary conditions and the reinforcement configuration. Here the Polymer is indicated with a light brown colour, while the CF with a dark green.

The specimen is subjected to tensile loading by means of vertical displacement application (see boundary conditions in Fig. 6). The geometry has been partitioned to take into account the presence of two materials, i.e. the polymer and the CF. The properties of these two materials are the same for the specimen studied in Section 3. In all the cases, a mesh constituted by Plane Stress Abaqus triangular and quadrilateral linear elements has been used. The Phase Field analysis has been carried out as in the previous section.

4.2. Results

In the following subsections, the results of the numerical simulations performed with different models are shown. In the first part, the numerical correlation with the experiment performed in [10] is shown, thus ensuring the ability of Phase Field to correctly catch the crack pattern. Later, a comparison of different reinforcement patterns is performed, both in terms of crack path and mechanical response of the coupon.

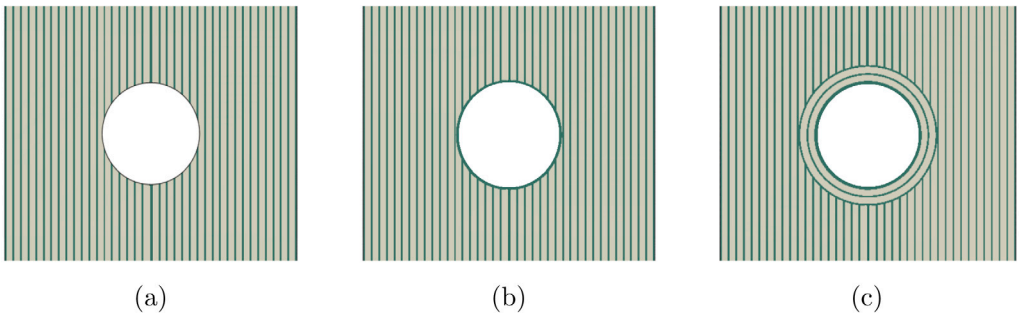

Fig. 8. Different reinforcement geometries.

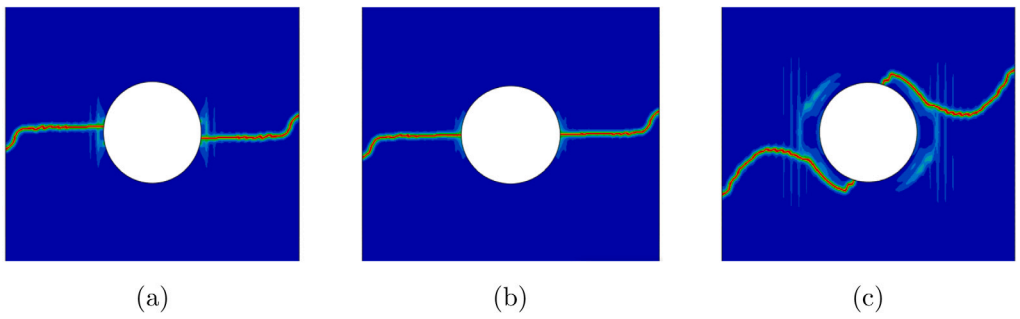

Fig. 9. Different reinforcement geometries and crack patterns.

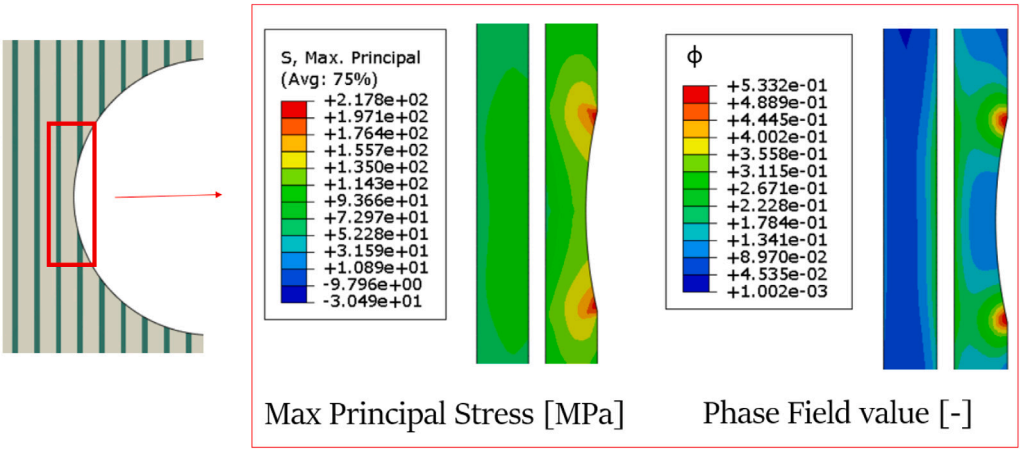

Fig. 10. Detail of the Principal Stress and Phase Field values at the interface of Matrix and Fibre for configuration 'a'.

4.2.1. Reinforced Open Hole specimen: comparison with experimental results

The results of the analysis show good agreement with the experiments performed by [10], as far as the crack pattern is concerned (Fig. 7).

The crack starts propagating from the outer boundaries and continues cutting the vertical CFs. Once it reaches the circular reinforcement around the hole, it follows the weaker part around the most external circular CF reinforcement, i.e. the one where only the polymeric material is present, exactly as it happened in the tensile specimen analysed in Section 3.2.2. In the numerical simulation a symmetric crack is present due to the perfect symmetry of the model. Instead, in the experimental work only one path is present, probably due to manufacturing defects that lead to particular higher stress concentration regions.

4.2.2. Reinforced Open Hole specimen: different reinforcement geometries

A comparison of different reinforcement patterns is carried out, highlighting the difference that small changes in the CF deposition path have on the crack pattern and overall response of the specimen. Different geometries are taken into consideration, taking into account the different manufacturing solutions that could be adopted. The analysed configurations are shown in Fig. 8.

This highlights the possible configurations that could be considered instead of the one used in Section 4.1. The first reinforcement geometry, 'a', is the classical one obtained with a simple drilling of the specimen after the deposition of the CF and Polymer. This is the reinforcement geometry which would be obtained following the main process of fabrication in the aeronautical industry: prepreg laying up, curing and machining the hole. In this way, the CF does not follow the contour of the hole but is simply cut as a result of the manufacturing operation. The other configurations ('b' and 'c'), as can be noticed, differ only a little bit between them, basically considering a different number of circular reinforcements around the hole or the connection between the straight CF and the circular one.

In Fig. 9 the different crack patterns resulting from the simulations are shown. In the first two cases (configuration 'a' and configuration 'b')

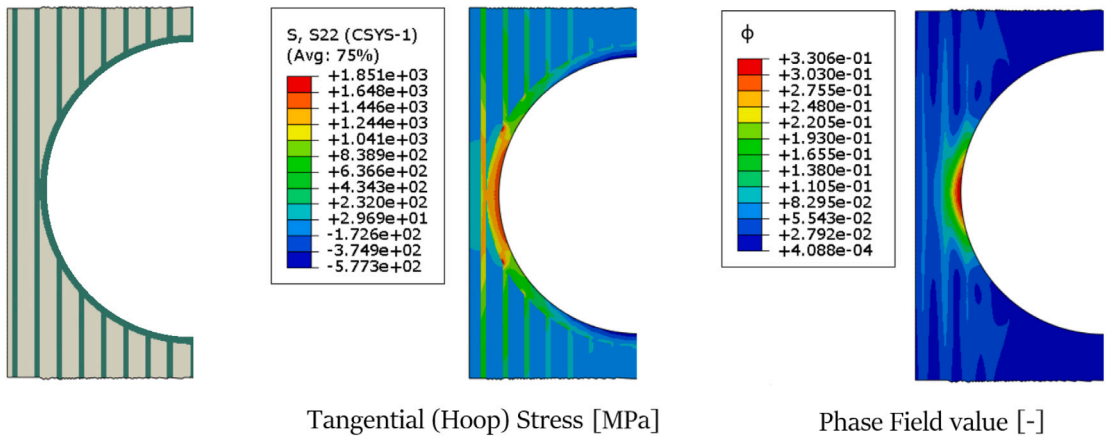

Fig. 11. Detail of the Hoop Stress and Phase Field values at the hole boundary for configuration 'b'.

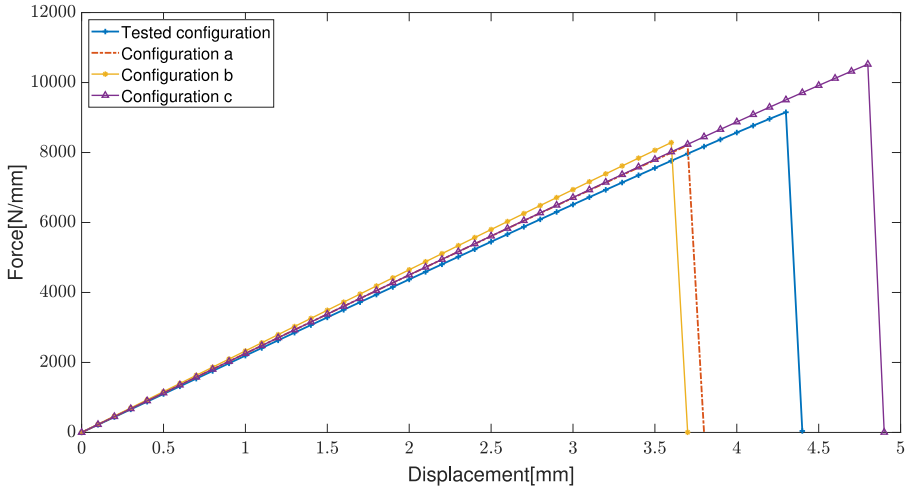

Fig. 12. Holed specimen: comparison among different reinforcement geometries.

the crack starts from the hole and cuts the specimen. In configuration 'a' in particular, the two crack branches are not aligned due to the presence of fibres cut at the edge of the hole itself. Due to the material discontinuity, there is a concentration of stress that leads to the crack propagation from that point. This can be fully appreciated in Fig. 10, where the material discontinuity is highlighted, along with the plot of the maximum principal stress for the matrix and the respective Phase Field values. As can be noticed, the presence of the interface between two materials at the boundary of the hole creates a stress concentration in the matrix region that promotes the crack propagation from that point. That is the reason why the crack does not propagate from the symmetry axis of the hole but with a small offset, justified by the presence of such discontinuity.

The same analysis performed for configuration 'a' is here done for configuration 'b'. Here the hole has a layer of circular CF reinforcement, avoiding stress concentrations at the interface between straight fibres and the matrix (which is the case of reinforcement 'a'), thus leading to a crack propagation aligned with the axis of symmetry of the hole. In fact, having a look at Fig. 11, it is very easy to notice that the maximum shear (hoop) stress around the hole is in correspondence of its symmetry axis. To this maximum vale corresponds a high value for the Phase Field, thus leading to a symmetric crack propagation from the symmetry axis.

In 'c' a phenomenon similar to what happened in the previous section takes place. The crack follows the path designed with the 3D printer, not originating from the hole, thus underlining the beneficial effect of the reinforcement around the stress concentration point. Different geometries for the reinforcement correspond to different mechanical response, as highlighted in Fig. 12. In any case, the beneficial contribution of the circular CF reinforcements around the hole is evident. In fact, the two specimens with multiple layers reinforcement can sustain a higher load before failing with respect to the ones with no or just single layer reinforcement. It is also worth noticing the importance of the fibre connection. In case the straight fibres are chopped, the mechanical response is less efficient with respect to the case where these fibres are joined to the circular ones, thus not letting the crack find a low resistance path through the sole matrix. As final remark, the same effect of the CF on the mechanical stiffness highlighted in Section 3.3 can be appreciated. Higher the percentage of CF reinforcement aligned with the loading direction, higher the stiffness of the coupon.

5. Concluding remarks

In this work, Phase Field fracture modelling has been used to predict the fracture behaviour of 3D printed materials reinforced by means of continuous CF deposition. In the first part, experiments already performed by other authors have been used to check the capability of this technique to capture the crack behaviour, finding good agreement with the experiments both in terms of crack pattern and mechanical response.

In a second part, the analysis has been extended to the Open Hole tension specimen, analysing the differences in crack pattern and mechanical response of different reinforcement geometries. In both the cases analysed, the beneficial effect of the CF reinforcement around

the stress concentration regions (in this case notches and holes) is highlighted. The capability of Phase Field to catch the fracture pattern could pave the way to a load-driven reinforcement geometry strategy, in order to obtain tougher structures, more resistant to fracture phenomena, by means of accurate CF deposition around the stress concentration regions.

A new experimental campaign is planned in order to check the validity of the new load-driven designs. In addition, manufacturing limitations in the CF reinforcement geometry could be included in the analysis. These limitations would add some constraints which could modify the optimum reinforcement geometry in order to make feasible its fabrication. Further analyses regarding the material properties have to be carried out, especially regarding the CF bundle. Being this one the main structural material in the 3D printed specimen, it is important to clearly assess its mechanical properties through ad-hoc experiments, due to the lack of data in the literature.

CRediT authorship contribution statement

S. Sangaletti: Conceptualization, Data curation, Methodology, Investigation, Formal analysis, Writing – original draft. **I.G. García:** Supervision, Conceptualization, Writing – review & editing.

Declaration of competing interest

The authors declare the following financial interests/personal relationships which may be considered as potential competing interests: Simone Sangaletti reports financial support was provided by European Commission. Israel Garcia Garcia reports financial support was provided by European Commission.

Data availability

Data will be made available on request.

Acknowledgements

This project has received funding from the European Union's Horizon 2020 research and innovation programme under the Marie Skłodowska-Curie grant agreement No 861061—NEWFRAC Project.

References

[1] Kumar HP, Xavior MA. Graphene reinforced metal matrix composite (GRMMC): A review. Procedia Eng 2014;97:1033–40, "12th Global Congress on Manufacturing and Management" GCMM - 2014.
[2] Pertuz AD, Díaz-Cardona S, González-Estrada OA. Static and fatigue behaviour of continuous fibre reinforced thermoplastic composites manufactured by fused deposition modelling technique. Int J Fatigue 2020;130:105275.
[3] Caminero MA, Chacón JM, García-Moreno I, Reverte JM. Interlaminar bonding performance of 3D printed continuous fibre reinforced thermoplastic composites using fused deposition modelling. Polym Test 2018;68:415–23.
[4] Caminero M, Chacón J, García-Moreno I, Rodríguez G. Impact damage resistance of 3D printed continuous fibre reinforced thermoplastic composites using fused deposition modelling. Composites B 2018;148:93–103.
[5] Justo J, Távara L, García-Guzmán L, París F. Characterization of 3D printed long fibre reinforced composites. Compos Struct 2018;185:537–48.
[6] Dutra TA, Ferreira RTL, Resende HB, Guimarães A. Mechanical characterization and asymptotic homogenization of 3D-printed continuous carbon fiber-reinforced thermoplastic. J Braz Soc Mech Sci Eng 2019;41(3):1–15.
[7] Akasheh F, Aglan H. Fracture toughness enhancement of carbon fiber–reinforced polymer composites utilizing additive manufacturing fabrication. J Elastomers Plast 2019;51(7–8):698–711.
[8] Saeed K, McIlhagger A, Harkin-Jones E, Kelly J, Archer E. Predication of the in-plane mechanical properties of continuous carbon fibre reinforced 3D printed polymer composites using classical laminated-plate theory. Compos Struct 2021;259:113226.
[9] Prajapati AR, Dave HK, Raval HK. Effect of fiber reinforcement on the open hole tensile strength of 3D printed composites. Mater Today Proc 2021;46:8629–33.
[10] Sanei SH, Arndt A, Doles R. Open hole tensile testing of 3D printed continuous carbon fiber reinforced composites. J Compos Mater 2020;54(20):2687–95.
[11] Jiang D, Hoglund R, Smith DE. Continuous fiber angle topology optimization for polymer composite deposition additive manufacturing applications. Fibers 2019;7(2).
[12] Safonov AA. 3D topology optimization of continuous fiber-reinforced structures via natural evolution method. Compos Struct 2019;215:289–97.
[13] Li P, Yvonnet J, Combescure C, Makich H, Nouari M. Anisotropic elastoplastic phase field fracture modeling of 3D printed materials. Comput Methods Appl Mech Engrg 2021;386.
[14] Yin B, Zhang L. Phase field method for simulating the brittle fracture of fiber reinforced composites. Eng Fract Mech 2019;211:321–40.
[15] Bourdin B, Francfort G, Marigo J-J. The variational approach to fracture. J Elasticity 2008;91(1):5–148.
[16] Miehe C, Hofacker M, Welschinger F. A phase field model for rate-independent crack propagation: Robust algorithmic implementation based on operator splits. Comput Methods Appl Mech Engrg 2010;199(45):2765–78.
[17] Guillén-Hernández T, Quintana-Corominas A, García IG, Reinoso J, Paggi M, Turón A. In-situ strength effects in long fibre reinforced composites: A micromechanical analysis using the phase field approach of fracture. Theor Appl Fract Mech 2020;108.
[18] Zhang P, Hu X, Yang S, Yao W. Modelling progressive failure in multi-phase materials using a phase field method. Eng Fract Mech 2019;209:105–24.
[19] Zhang P, Yao W, Hu X, Bui TQ. 3D micromechanical progressive failure simulation for fiber-reinforced composites. Compos Struct 2020;249:112534.
[20] Tan W, Martínez-Pañeda E. Phase field predictions of microscopic fracture and R-curve behaviour of fibre-reinforced composites. Compos Sci Technol 2021;202:108539.
[21] Tan W, Martínez-Pañeda E. Phase field fracture predictions of microscopic bridging behaviour of composite materials. Compos Struct 2022;286:115242.
[22] Dean A, Asur Vijaya Kumar P, Reinoso J, Gerendt C, Paggi M, Mahdi E, Rolfes R. A multi phase-field fracture model for long fiber reinforced composites based on the puck theory of failure. Compos Struct 2020;251:112446.
[23] Asur Vijaya Kumar P, Dean A, Reinoso J, Lenarda P, Paggi M. Phase field modeling of fracture in functionally graded materials: Γ-convergence and mechanical insight on the effect of grading. Thin-Walled Struct 2021;159:107234.
[24] Francfort G, Marigo J-J. Revisiting brittle fracture as an energy minimization problem. J Mech Phys Solids 1998;46(8):1319–42.
[25] Ambrosio L, Tortorelli VM. Approximation of functional depending on jumps by elliptic functional via t-convergence. Comm Pure Appl Math 1990;43(8):999–1036.
[26] Ambrosio L, Tortorelli VM. On the approximation of free discontinuity problems. Boll Mater Ital B 1992;7(6):105–23.
[27] Kuhn C, Schlüter A, Müller R. On degradation functions in phase field fracture models. Comput Mater Sci 2015;108:374–84.
[28] Klinsmann M, Rosato D, Kamlah M, McMeeking RM. An assessment of the phase field formulation for crack growth. Comput Methods Appl Mech Engrg 2015;294:313–30.
[29] Kristensen P, Niordson C, Martínez-Pañeda E. An assessment of phase field fracture: crack initiation and growth. Philos Trans R Soc Lond Ser A Math Phys Eng Sci 2021;379:2203.
[30] Navidtehrani Y, Betegón C, Martínez-Pañeda E. A unified abaqus implementation of the phase field fracture method using only a user material subroutine. Materials 2021;14(8):1–19.
[31] Cuesta I, Martinez-Pañeda E, Díaz A, Alegre J. The essential work of fracture parameters for 3D printed polymer sheets. Mater Des 2019;181.
[32] Camanho P, Maimí P, Dávila C. Prediction of size effects in notched laminates using continuum damage mechanics. Compos Sci Technol 2007;67(13):2715–27.